

Doping dependence of the low-energy excitations in superconducting $\text{Bi}_2\text{Sr}_2\text{CaCu}_2\text{O}_{8+\delta}$: Evidence for thermal phase fluctuations

G. Lamura,^{1,*} J. Le Cochech,^{1,†} A. Gauzzi,² F. Licci,² D. Di Castro,³ A. Bianconi,³ and J. Bok¹¹Laboratoire de physique du solide, ESPCI 10, rue Vauquelin, 75231 Paris, France²Istituto Materiali per Elettronica e Magnetismo - Consiglio Nazionale delle Ricerche Area delle Scienze, 43010 Parma, Italy³Dipartimento di Fisica and INFN, Università di Roma "La Sapienza" P.le Aldo Moro 4, 00185 Roma, Italy

(Received 27 March 2002; revised manuscript received 9 August 2002; published 28 April 2003)

By using a single-coil technique, we study the low-temperature dependence of the in-plane magnetic penetration depth λ_{ab} in several $\text{Bi}_2\text{Sr}_2\text{CaCu}_2\text{O}_{8+\delta}$ (BSCCO) single crystals prepared with various doping levels δ ranging from the under- to the overdoped regime. Four samples exhibit a linear dependence of thermally activated low-energy excitations $\Delta\lambda_{ab} \equiv \lambda_{ab}(T) - \lambda_{ab}(0) \sim T$. The thermal activation rate $\propto \partial\lambda_{ab}/\partial T$ is minimum, 8 Å/K, at optimum doping, in good quantitative agreement with the d -wave model of superconducting order parameter. The much larger rates, ≥ 40 Å/K, observed in all under- and overdoped samples indicate that, in these samples, another type of low-energy excitations is relevant. These large rates are quantitatively consistent with a model of thermal phase fluctuations suitable for granular superconductors with short coherence length like cuprates. One underdoped sample exhibits a quadratic dependence suggesting an incipient crossover from thermal to quantum fluctuations.

DOI: 10.1103/PhysRevB.67.144518

PACS number(s): 74.25.Nf, 74.40.+k, 74.72.Hs

I. INTRODUCTION

A large body of experimental data gives evidence that the superconducting CuO_2 planes of cuprates are *intrinsically* granular in the nm scale.^{1–6} A striking evidence was recently provided by high-resolution scanning tunnelling spectroscopy on $\text{Bi}_2\text{Sr}_2\text{CaCu}_2\text{O}_{8+\delta}$ (BSCCO) single crystals^{3–5} and confirmed on thin films.⁶ The emerging picture is that hole-rich and hole-poor domains, with size of the order of the in-plane superconducting coherence length, coexist in the superconducting planes. The former domains are expected to be metallic and superconducting, while the latter ones may be nonsuperconducting and antiferromagnetic or with strong residual antiferromagnetic fluctuations. Such *electronic* inhomogeneities are not to be confused with *chemical* inhomogeneities or disorder.

To investigate the role of the above inhomogeneities on the low-energy spectrum in cuprates, here we report on the low-temperature behavior of the in-plane magnetic penetration depth λ_{ab} in BSCCO single crystals as a function of doping δ . Indeed, doping was found to strongly affect the domain formation.⁴ Our results suggest that in both under- and overdoped regimes the statistical weight of zero-energy excitations leading to a linear temperature dependence of λ_{ab} at low temperature is much larger than that predicted by a simple d -wave model.^{7–9} Such extra excitations are quantitatively accounted for by a simple model of thermal phase fluctuations of the order parameter. This model is known to be appropriate for granular systems like cuprates.

II. EXPERIMENT

A. Single-crystal preparation and doping

We studied five BSCCO single crystals (see Table I): one optimally doped, labeled as "Op," three underdoped, "Ar," "R1," and "R2," and one overdoped, "Ox," with supercon-

ducting critical temperatures $T_c = 92, 83, 74, 75,$ and 80 K, respectively. The Ox sample is in fact the Op sample which was subsequently annealed in oxygen to overdope it, as described below. Op and Ar were grown from a high-temperature solution, as described in detail elsewhere.¹⁰ In summary, we used a peritectic reaction from self-fluxed, partial-melted stoichiometric powders. Bi_2O_3 , BaCO_3 , SrCO_3 , and CuO were weighted, homogenized, hand pressed in a platinum crucible, and subsequently covered with a well-sticking lid. The crucible was heated at 920°C in air, soaked for 30 h, cooled at 2°C/h down to 780°C and finally removed from the furnace. The resulting porous mass could be easily separated from the crucible and cleaved to obtain crystalline sheets of cm size. From these sheets we separated platelet-shaped single crystals of mm size in the ab plane and 0.1-mm-size thick. Two as-grown crystals of the same batch were selected for their good crystalline properties with no trace of intergrowths. X-ray-diffraction rocking curve analysis shows narrow peaks with full width at half maximum of $\approx 0.23^\circ$ for the (0 0 20) peak. As expected, the crystal symmetry is tetragonal with lattice parameters $a = b = 5.413$ Å and $c = 30.893$ Å. The ratios of cation composition Bi:Sr:Ca:Cu were measured by means of energy-dispersive x-ray analysis (EDAX), which yielded $2.14 \pm 0.04:2.00 \pm 0.02:1.00 \pm 0.01:1.86 \pm 0.02$. The onset T_c measured by means of the single-coil technique described in the following section was ≈ 92 K, which indicates that these as-grown crystals are optimally doped. The remaining two crystals used for this study, R1 and R2, were selected from the same batch grown by the traveling-solvent floating-zone technique using an infrared radiation furnace.^{11,12} Typical size and weight of the samples cut from the crystal boules were respectively $\approx 1.4 \times 1.4 \times 0.05$ mm³ and 0.5 mg. In samples R1 and R2 the ratios of cation composition as measured by means of EDAX were found to be 2.13:2.02:0.88:1.97, i.e. samples R1 and R2 are less Cu de-

TABLE I. Sample characteristics and comparison between experimental and predicted values of $\partial\lambda_{ab}/\partial T$. The latter values are obtained by taking $\lambda_{ab}(0)|_{\eta=0} = 2500 \text{ \AA}$ [Refs. 20, 30, and 31 in Eqs. (3), (4), and (6)]. The doping level η is estimated from the empirical relation (Ref. 16) $T_c/T_c^{MAX} \approx 1 - 82.6\eta^2$. The Δ_0 values are taken from Andreev reflection and Raman scattering data, which both yield $2\Delta_0/k_B T_c = 5-6$ (Ref. 24).

Sample	R1	R2	Ar	Op	Ox
Annealing	argon	argon	argon	as-grown	oxygen
T_c [K]	73.8	74.8	83	92	80.4
ΔT_c [K]	8	5.3	6	1.3	4
η	-0.049	-0.048	-0.034	0	0.039
$2\Delta_0/k_B T_c$	6	6	6	5	6
$\partial\lambda_{ab}/\partial T$ exp. [$\text{\AA}/\text{K}$]	59.4		42.4	7.8	47
$\partial\lambda_{ab}/\partial T$ <i>d</i> -wave [$\text{\AA}/\text{K}$]	9	8	7	8	8
$\partial\lambda_{ab}/\partial T$ phase fluct. [$\text{\AA}/\text{K}$]	57	56	47	41	50

efficient and more Ca deficient than Op, Ar, and Ox. As for the previous crystals, x-ray diffraction was used to control the crystal quality and yielded $a=b=5.413 \text{ \AA}$ and $c=30.90 \text{ \AA}$. In order to obtain over- or underdoped samples, the as-grown crystals were annealed in flowing oxygen (sample Ox) or argon (samples Ar, R1, and R2) respectively, at 600 or at 900 °C for about 140 h, as described elsewhere.^{10,13-15} From Table I we see that both types of treatments produced significant T_c reductions, which is a first indication of over- or underdoping. This indication was confirmed by iodometric titration analysis¹⁰ on sintered samples to which the same annealing treatments were applied. This analysis was not applicable to the single crystals, since samples as big as 200–300 mg or more are required. However, the large number of samples studied let us conclude that the qualitative result of this analysis is valid for the single crystals as well. The lower T_c of the R1 and R2 samples can be explained by the lower average doping level of Cu as a consequence of the higher Cu content. In the following we assign to each sample the doping level p as derived from a well-established empirical relation between T_c and p .¹⁶

B. Single-coil technique for T_c and λ_{ab} measurements

The temperature dependence of the in-plane magnetic penetration depth $\lambda_{ab}(T)$ was measured on freshly cleaved single crystals using a single coil-mutual inductance technique described in detail elsewhere.¹⁷ In summary, the principle of operation of this technique is based on the change of inductance of a miniaturized pancake coil located in the proximity of the superconducting sample. This change is detected as a change of the resonant frequency f of an *RLC* circuit formed by the coil in parallel with a low-loss capacitor and kept at 4.2 K. A high-stability marginal oscillator is used to measure f that depends on the circuit parameters according to the relation

$$f = \frac{1}{2\pi} \sqrt{\frac{1}{L(T)C} - \left[\frac{R(T)}{L(T)}\right]^2}, \quad (1)$$

where C is the capacitance and L and R are the coil inductance and coil resistance, respectively. In Eq. (1), it is explicitly indicated that L and R depend on the temperature-dependent sample response. The sample contribution to R is usually negligible except in the transition region, where sample losses can be important. At sufficiently low temperature and for sufficiently low coil excitation currents, the electrodynamic response is adequately described by the London regime, i.e. the response is linear, mostly diamagnetic, and the losses are negligible. Our measurements are restricted to this simple case, where the variation of coil inductance takes the following closed form

$$\Delta L = L_0 - L = \pi\mu_0 \int_0^\infty \frac{M(\gamma)d\gamma}{1 + 2\gamma\lambda_{ab} \coth(d/\lambda_{ab})}, \quad (2)$$

where d is the sample thickness and $M(\gamma)$ is a function of the spatial frequency γ . M depends only on the coil geometry and on the sample-coil distance. Typical frequency and magnitude of the electromagnetic (e.m.) field perpendicular to the sample surface are 2–4 MHz and <0.1 mT, respec-

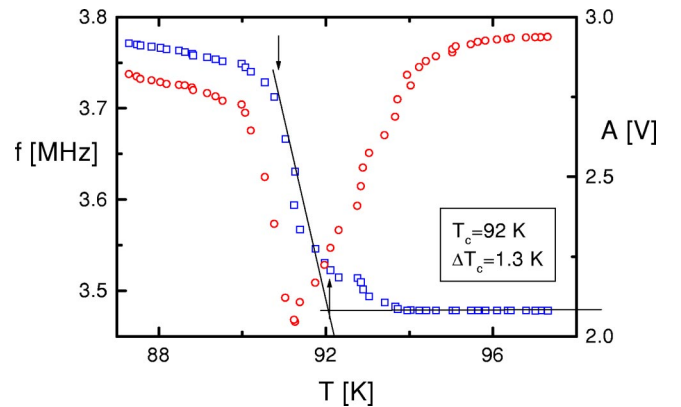


FIG. 1. T_c characterization of the optimally doped, Op, sample using the single-coil technique described in the text. Note at the transition the change of the resonant frequency f (\square) of the circuit coupled to the superconductor and of the oscillation amplitude A (\circ). The arrows indicate the width of the superconducting transition. The solid lines are a guide for the eye.

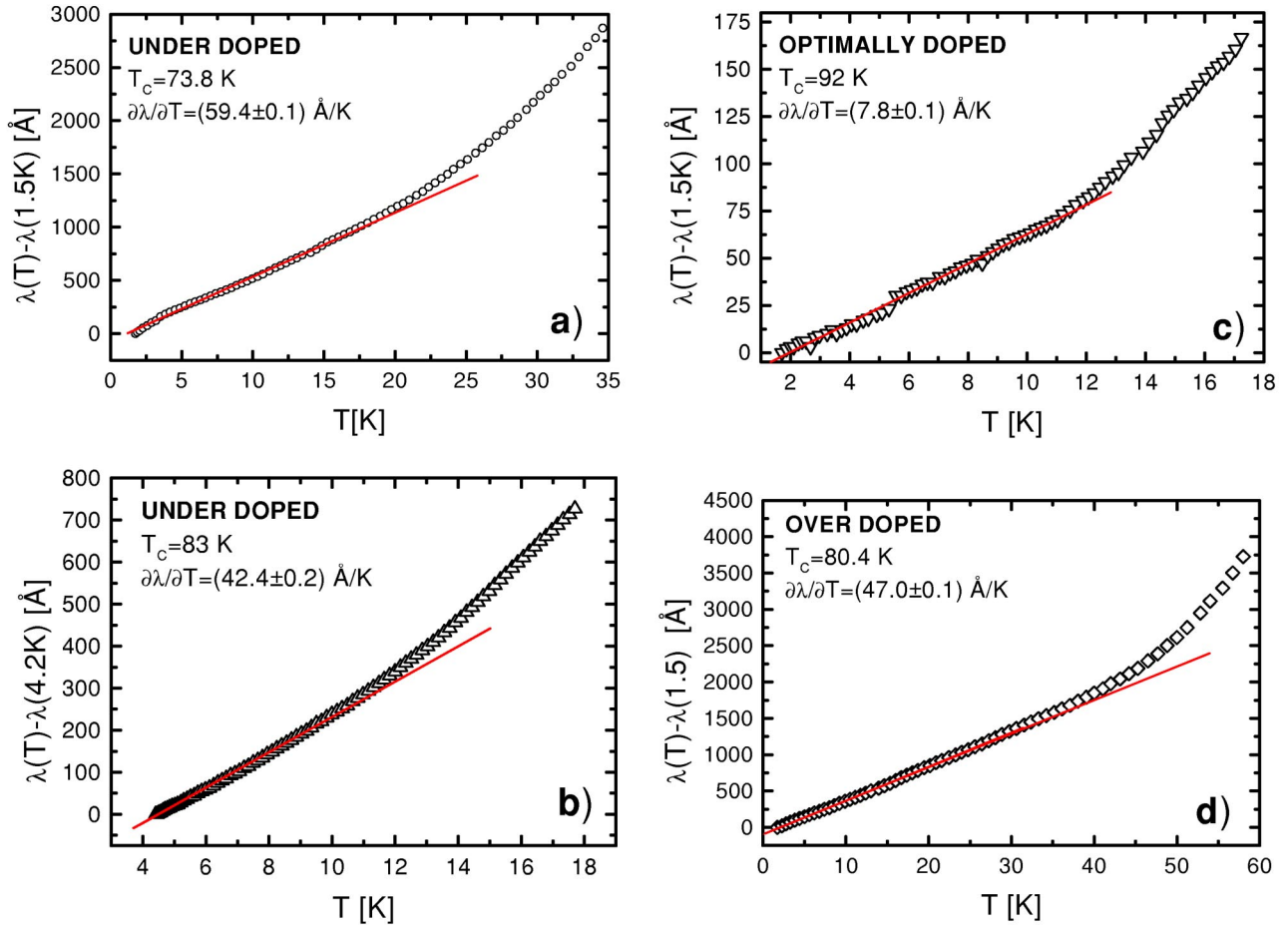


FIG. 2. Low-temperature dependence of $\Delta\lambda_{ab}$ of the four BSSCO crystals (a) R1, (b) Ar, (c) Op, and (d) Ox displaying a predominantly linear behavior. The main sample characteristics are described in the text and in Table I. The solid lines are a guide for the eye. The deviations from the linearity in (a) are discussed in the text.

tively. We verified to operate always in the linear-response regime, i.e., below the first critical field, by varying the coil current. We also verified the absence of edge effects that the small crystal size may cause. To do this we measured¹⁸ an even smaller high quality optimally doped YBCO single crystal¹⁹ and obtained the same value of linear increase $\partial\lambda(T)/\partial T = 4.5 \text{ \AA/K}$ at low temperature reported previously.⁹ The absence of edge effects in our case is supported by numerical simulations¹⁸ of the spatial decay of the e.m. field generated by the coil. These simulations suggest that no significant edge effects are expected in samples equal or larger than two times the coil diameter.

III. T_c AND λ_{ab} RESULTS

In Fig. 1, we report the typical behavior of f in the transition region. Note the abrupt increase at T_c caused by the screening supercurrents that reduce the coil inductance, according to Eq. (1). In an homogeneous sample, the onset of such inductive transition coincides with the zero-resistance transition, at which macroscopic loops of supercurrents are formed. In Fig. 1 we also show the change of amplitude A of the oscillating signal at T_c . This amplitude varies as the quality factor Q of the resonant circuit. The diplike behavior

of A at the transition is mainly due to vortex dissipation. In Figs. 2 and 3 we report the low-temperature dependence of the variation $\Delta\lambda_{ab}(T) \equiv \lambda_{ab}(T) - \lambda_{ab}(0)$ for all samples. These curves are obtained from the raw f -data using Eqs. (1) and (2), as described in Ref. 17.

In Table I we summarize the main characteristics of each sample: T_c , transition width ΔT_c , and low-temperature slope $\partial\lambda_{ab}/\partial T$. T_c was conventionally defined as the intersection of the tangent to the $f(T)$ curve in the normal state with the tangent at the inflexion point. Four samples R1, Ar, Op, and Ox display a predominantly linear dependence, $\Delta\lambda_{ab} \sim T$, up to 12–40 K, depending on the sample (see Fig. 2). The main point on which we focus is that these measurements show a strong dependence of the slope upon doping. In the optimally doped sample Op, we find 8 \AA/K , in agreement with previously published data.^{20,21} Much larger values, $\approx 40 \text{ \AA/K}$, are observed in both the under- and the over-doped samples R1, Ar, and Ox. In the curve of R1 it appears a downturn at 3 K that may suggest the presence of proximity effects caused by metallic phases in the nm scale.²² A detailed discussion regarding the temperature dependence of the gapless behaviors of Fig. 2(a) goes beyond the scope of this work. We shall limit ourselves to discuss the origin of

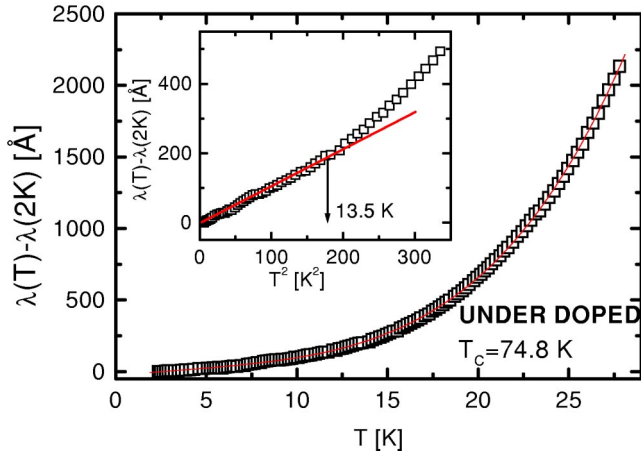


FIG. 3. The same as in Fig. 2 for the sample R2, the only underdoped crystal displaying a nonlinear dependence of $\Delta\lambda_{ab}$. The solid line is the fourth-order polynomial fit. In the inset the data are plotted as a function of T^2 . The solid line is a guide for the eye and puts into evidence the quadratic dependence below $T^\dagger = 13.5$ K.

the *average* number of thermally activated zero-energy excitations evidenced by the above predominantly linear dependence.

The remaining sample, i.e., the underdoped sample R2, exhibits a superlinear temperature dependence approximated by a quadratic dependence below ≈ 13.5 K with curvature ≈ 1.06 Å/K² (see Fig. 3). The latter value is in good agreement with a previous study reporting a similar quadratic behavior in BSCCO crystals.²³

IV. ANALYSIS OF λ_{ab} DATA

A. *d*-wave model

We first analyze the above results within the framework of the ordinary *d*-wave model currently adopted for cuprates. According to this model, the temperature dependence of λ_{ab} , which is proportional to the fraction of normal electrons in the low-temperature limit, follows a linear dependence with slope,^{7,8}

$$\frac{\partial\lambda_{ab}}{\partial T} \approx \ln 2k_B \frac{\lambda_{ab}(0)}{\Delta_0}, \quad (3)$$

where Δ_0 is the zero-temperature superconducting gap, not to be confused with the pseudogap. As pointed out by Deutscher,²⁴ these two gaps represent two different energy scales and are therefore probed by different techniques. The former gap can be typically measured by Andreev reflection or by Raman scattering. For BSCCO crystals, various authors consistently report $\Delta_0 \approx 2.5 - 3k_B T_c$, with no sizeable doping dependence.²⁴⁻²⁶ The experimental values of $\lambda_{ab}(0)$ reported for Bi2212 crystals are in the 1700–3000-Å range.^{21,27-31} This discrepancy mostly arises from the different experimental techniques used and from the various methods of data analysis that often require *a priori* the validity of the two-fluid model or of the BCS weak-coupling limit, for instance. In fact only the restricted range of 2500–2700 Å is

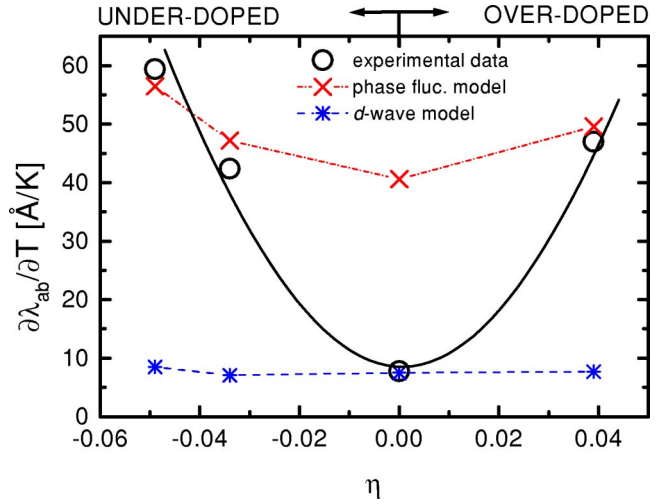


FIG. 4. Doping dependence of the low-temperature slope $\partial\lambda_{ab}/\partial T$ obtained from the data of Fig. 2. The dash line and (*) represent the *d*-wave model prediction of Eq. (3); the dash-dot line and (×) represent the prediction of the phase fluctuation model; the open circles represent the experimental data; the solid line is a guide for the eye showing the proposed crossover from the *d*-wave regime in the optimally doped region to the phase fluctuation regime in the under- and overdoped regions.

compatible with the interpretation of the experimental slope values within *d*-wave model for optimally doped BSCCO, as commonly accepted.^{20,29-31} Within this range, our data analysis is insensitive to the particular value used. To fix the ideas we used the value of 2500 Å, which is also in agreement with the strong-coupling value 2.5 that accounts for the spectroscopic data of BSCCO.²⁴ In Eq. (3) we include the doping dependence of $\lambda_{ab}(0)$ by using the empirical relations reported in Refs. 16 and 30–36,

$$\lambda_{ab}(0) = \lambda_{ab}(0)|_{\eta=0} (1 - 82.6\eta^2)^{-1/2}, \quad (4)$$

where $\eta \equiv p - p_{opt}$ represents the departure of the doping p from the optimum value, p_{opt} . We note that the uncertainty of the values predicted by Eqs. (3) and (4) is less than 20%, arising from the aforementioned uncertainty in the determination of Δ_0 and of $\lambda_{ab}(0)$. The uncertainty in the experimental values is less than 0.1 Å/K, as indicated by the linear regression of the experimental points. By applying Eqs. (3) and (4) to our results (see Table I and Fig. 4), a good agreement between experimental values and predicted ones is obtained only for the optimally doped sample Op. For both the under- and the overdoped samples, the values predicted by the *d*-wave model are, on average, at least five times smaller than the experimental ones. This conclusion is unchanged after taking into account that Eq. (3) must be corrected if the angular dependence of the gap function, $\Delta(\varphi)$, contains higher-order harmonics. Indeed, the prefactor of Eq. (3) scales as the inverse of the slope of the gap function at the node position.³⁷ Using the experimental slope values measured by ARPES (Ref. 38) as a function of doping, it turns out that the prediction of Eq. (3) would be corrected by 20% or less at any doping level.

The case of R2, the only sample exhibiting a nonlinear temperature dependence, will be separately discussed in Sec. IV D.

B. Phase fluctuation picture

The data analysis reported before shows that the d -wave model fails to account for the large experimental slopes, $\partial\lambda_{ab}/\partial T$, found in the under- and overdoped regions. In these regions, another type of zero-energy excitations must therefore coexist with those at the nodes of the d -wave gap. Following previous works,^{39–41} we shall consider a picture of longitudinal phase fluctuations of the order parameter (Goldstone modes). These fluctuations can be relevant in metals with high resistivities and/or low carrier densities and are enhanced by a granular structure. Cuprates fulfill both conditions particularly in the under- and overdoped regions; indeed, the so-called boomeranglike dependence of the superfluid density on doping, experimentally found by a number of groups,^{32–34,30,31,36} shows that, in these regions, the superfluid density is substantially lower than in the optimally doped region. The experimental evidence of an *intrinsic* electronic granularity in the superconducting CuO₂ planes has already been discussed in the introduction.

In conclusion, we expect that classical or quantum fluctuations are relevant to our case. The latter fluctuations would dominate at sufficiently low temperature or in small grains (i.e., when the charging energy is sufficiently high). Both discrete or continuous models have been successfully applied to conventional granular superconductors like NbN (Ref. 42) and cuprates.⁴⁰ For our BSCCO crystals we shall adopt a continuous model of phase fluctuations in the ab plane. Indeed, according to the aforementioned scanning tunnel microscope studies,⁴ these crystals are viewed as a *chemically* homogeneous medium (i.e., without grain boundaries and/or intergranular phases) but with relevant *intrinsic electronic* inhomogeneities. To explain the linear dependence of λ_{ab} in our samples, we shall neglect quantum fluctuations in view of the following consideration. Theoretical studies^{41,43,44} supported by numerical calculations⁴⁰ predict that quantum fluctuations would lead to a reduction of the renormalized superfluid density. This would manifest itself as a progressive flattening of the $\lambda_{ab}(T)$ curves as $T \rightarrow 0$ K. This feature has never been observed in the curves of Fig. 2 which show a linear temperature dependence down to 1.5 K.

Phase fluctuations (if any) *coexist* with the usual quasiparticle BCS excitations. Both types of excitations lead to a progressive reduction of the superfluid density (hence to an increase of λ_{ab}) as temperature increases. In the case of classical phase fluctuations and in the Gaussian approximation, valid at low temperature and in the absence of dissipation, only long-wavelength longitudinal fluctuations of arbitrarily small energy are created. According to previous studies,^{40,39,41} this phenomenon produces the linear increase $\Delta\lambda_{ab} \sim T$ reported in Fig. 2.

C. Analysis of the $\lambda_{ab}(T)$ data within the phase fluctuation model

In order to quantitatively analyze the data of Table I using the above picture, we generalize the analytical expression for

the slope $\partial\lambda_{ab}/\partial T$ proposed by Roddick and Stroud⁴⁰ to the case of an anisotropic continuous medium suitable for cuprates. Within the Gaussian approximation, we obtain⁴⁵

$$\frac{\partial\lambda_{ab}(0)}{\partial T} \approx \frac{\mu_0 k_B}{\Phi_0^2} \frac{\lambda_{ab}^3(0)}{\xi_{ab}(0)} \gamma, \quad (5)$$

where Φ_0 is the flux quantum, ab and c indicate the ab plane and c axis, respectively, γ is the anisotropy factor, and $\xi_{ab}(0)$ is the in-plane coherence length at zero temperature. As in the previous case of the d -wave model, in Eq. (5) we take into account the doping dependence of $\lambda_{ab}(0)$ expressed by Eq. (4). The application of Eq.(5) also requires the knowledge of γ and of $\xi_{ab}(0)$ for each sample. However, taking into account recent data,⁴⁶ we notice that, at low temperature, γ varies between 100 and 200 in the p range $p_{opt} \pm 0.04$ of interest in our case. Taking into account that γ also depends on temperature and on the degree of crystal perfection, for all samples we use the average γ value reported in optimally doped samples, $\gamma^{opt} \approx 160$, by various authors.^{46–48} We also neglect the doping dependence of $\xi_{ab}(0)$. Indeed, it is straightforward to see that $\xi_{ab}(0)$ varies by less than 20% upon doping because this quantity scales as the ratio between the Fermi momentum and the superconducting gap, which both decrease from under- to overdoping.^{49–51} Therefore we take for all samples the value reported at optimum doping $\kappa_c^{opt} \equiv \lambda_{ab}(0)|_{\eta=0} / \xi_{ab}^{opt}(0) \approx 100$. This value has been reproducibly obtained within 20% from magnetization measurements by various authors.^{47,52–54,21,55} We then rewrite Eq. (5) as follows:

$$\frac{\partial\lambda_{ab}}{\partial T} \approx \frac{\mu_0 k_B}{\Phi_0^2} \gamma^{opt} \kappa_c^{opt} \lambda_{ab}^2(0)|_{\eta=0} (1 - 82.6\eta^2)^{-3/2}. \quad (6)$$

Taking into account the preceding estimations, the uncertainty of the slope values $\partial\lambda_{ab}/\partial T$ estimated using the Eq. (6) is less than 50%. The important point is that, on average, these predictions account very well for the large slope values observed in both the over- and the underdoped samples.

D. Nonlinear dependence of $\lambda_{ab}(T)$

We finally discuss the case of sample R2, which exhibits a superlinear behavior of $\lambda_{ab}(T)$ (see Fig. 3). This different electrodynamic response with respect to that of sample R1, that belongs to the same batch, can be explained by a different amount of disorder and/or by an inhomogeneous charge density in the superconducting planes. Indeed, the critical temperature T_c and the transition width ΔT_c of samples R1 and R2 are also different (see Table I). In the following, we shall discuss various possible microscopic mechanisms leading to a superlinear behavior of $\lambda(T)$ in a d -wave superconductor:

(i) Nonlocal effects near the gap nodes⁵⁶ for magnetic fields perpendicular to the conducting planes, as in our case, would lead to a quadratic dependence below a characteristic temperature $T^* = [\xi_{ab}(0)\Delta_0]/[\lambda_{ab}(0)k_B]$. Using in this expression the aforementioned values, we estimate

$T^* \approx 2.3$ K. Since a quadratic dependence is observed below 13.5 K, nonlocal effects should not be relevant to our case.

(ii) Impurity scattering in the unitary limit would also lead to a quadratic dependence below $T^\dagger \approx 0.83 \sqrt{\Gamma \Delta_0 / k_B^2}$, where Γ is the scattering rate parameter proportional to the impurity concentration.^{57,58} From the literature, we take $\Delta_0 / k_B T_c = 2.5$ and a large scattering rate $\Gamma / (T_c k_B) = 0.018$.^{57,58} We then obtain $\partial \lambda_{ab} / \partial T^2 \approx 0.93 \text{ \AA} / \text{K}^2$ and $T^\dagger = 13.2$ K. Both values are compatible with the experimental curve of Fig. 3. However, the application of this model to this curve meets the following difficulty: from Fig. 3 we would estimate $T^\dagger = 13.5$ K, the temperature above which a deviation from the quadratic dependence is observed. Above this temperature, resonant impurity scattering would become negligible and the linear temperature dependence predicted by the *d*-wave model would be recovered, which is in contrast to the data.

(iii) Quantum fluctuations would be enhanced by disorder and/or by an inhomogeneous charge density which could be different in samples of the same batch like samples R1 and R2. Both phenomena tend to increase the charging energy in a granular system. As mentioned before, quantum phase fluctuations are expected to suppress the superfluid density at low temperature.^{43,44} This would produce a flattening of the $\lambda_{ab}(T)$ curve for $T \rightarrow 0$, in qualitative agreement with the experimental curve of Fig. 3. To support this hypothesis, it would be necessary to extend our λ_{ab} measurements to the zero-temperature limit, where quantum phase fluctuations are expected to lead to localization effects^{59,60} that should be visible as an upturn of the $\lambda_{ab}(T)$ curve.

V. CONCLUSIONS

We studied the low-temperature dependence down to 1.5 K of the in-plane magnetic penetration depth λ_{ab} of five

BSCCO single crystals prepared with various doping levels ranging from the under- to overdoped regime. In agreement with previous studies, four samples display a predominantly linear dependence, $\Delta \lambda_{ab} \sim T$, up to 40 K, which gives evidence of zero-energy excitations in the electronic spectrum. However, only the data on the optimally doped sample are quantitatively explained by a simple *d*-wave model. In the remaining two under- and overdoped samples, the slope values $\partial \lambda_{ab} / \partial T$ are largely underestimated by this model for any realistic parameter and additional mechanisms leading to zero-energy excitations must be invoked. The data analysis shows that a simple model of classical phase fluctuations quantitatively accounts for our results. These fluctuations would indeed be favored by electronic inhomogeneities in the superconducting CuO_2 planes, in agreement with previous reports giving evidence of an intrinsic granularity in these planes. One underdoped sample displays a nonlinear dependence approximated by a quadratic dependence below 13.5 K. The data analysis is consistent with an incipient transition from classical to quantum fluctuations favored by disorder or by an inhomogeneous charge distribution. A definite answer to this question would require to extend our measurements to lower temperatures.

ACKNOWLEDGMENTS

We are grateful to B. K. Chakraverty, B. Plaçaïs, G. Deutscher, P. J. Hirschfeld, and H. Raffy for fruitful discussions. We thank P. Mathieu and C. Delalande for making available their low-temperature cryostat and S. Zannella for making available the EDAX apparatus. We are grateful to T. Besagni, P. Ferro, and C. Orecchia for their valuable technical assistance.

*Corresponding author. Present address: INFN and Dipartimento Scienze Fisiche, Università di Napoli Federico II, I-80125, Napoli, Italy. Email address: gianrico.lamura@na.infn.it

[†]Present address: Laboratoire Pierre Süe, DRECAM, CEA-Saclay, 91191 Gif sur Yvette, France.

¹A.A.V.V., *Phase Separation in Cuprate Superconductors*, edited by K.-A. Müller and G. Benedek (World Scientific, Singapore, 1993).

²J. Mesot, P. Allenspach, U. Staub, A. Furrer, and H. Mutka, *Phys. Rev. Lett.* **70**, 3999 (1993).

³S. H. Pan, J. P. O'Neal, R. L. Badzey, C. Chamon, H. Ding, J. R. Engelbrecht, Z. Wang, H. Eisaki, S. Uchida, A. K. Gupta, K. W. Ng, E. W. Hudson, K. M. Lang, and J. C. Davis, *Nature (London)* **413**, 283 (2001).

⁴K. M. Lang, V. Madhavan, J. E. Hoffman, E. W. Hudson, H. Eisaki, S. Uchida, and J. C. Davis, *Nature (London)* **415**, 412 (2002).

⁵C. Howald, P. Fournier, and A. Kapitulnik, *Phys. Rev. B* **64**, 100504 (2001).

⁶T. Cren, D. Roditchev, W. Sacks, J. Klein, J.-B. Moussy, C. Deville-Cavellin, and M. Laguës, *Phys. Rev. Lett.* **84**, 147 (2000).

⁷F. Gross, B. S. Chandrasekhar, D. Einzel, K. Andres, P. J. Hir-

schfeld, H. R. Ott, J. Beuers, Z. Fisk, and J. L. Smith, *Z. Phys. B: Condens. Matter* **64**, 175 (1986).

⁸D. J. Scalapino, *Phys. Rep.* **250**, 329 (1995).

⁹W. N. Hardy, D. A. Bonn, D. C. Morgan, R. Liang, and K. Zhang, *Phys. Rev. Lett.* **70**, 865 (1993).

¹⁰F. Licci (unpublished).

¹¹G. D. Gu, K. Takamuku, N. Kodhizuka, and S. Tanaka, *J. Cryst. Growth* **130**, 325 (1993).

¹²A. Bianconi (unpublished).

¹³F. Jean, J.-F. Marucco, G. Collin, M. Andrieux, and N. Blanchard, *Supercond. Sci. Technol.* **13**, 1167 (2000).

¹⁴G. Briceno and A. Zettl, *Phys. Rev. B* **40**, R11 352 (1989).

¹⁵H. Raffy (private communication).

¹⁶M. R. Presland, J. L. Tallon, R. G. Buckley, R. S. Liu, and N. E. Flower, *Physica C* **176**, 95 (1991).

¹⁷A. Gauzzi, J. L. Cochee, G. Lamura, B. J. Jönsson, V. A. Gasparov, F. R. Ladan, B. Placais, P. A. Probst, D. Pavuna, and J. Bok, *Rev. Sci. Instrum.* **71**, 2147 (2000).

¹⁸J. L. Cochee, Ph.D. thesis, Paris VI, 1999.

¹⁹A. Erb, E. Walker, and Flükiger, *Physica C* **245**, 245 (1995).

²⁰T. Jacobs, S. Shridar, Q. Li, G. D. Gu, and N. Koshizuka, *Phys. Rev. Lett.* **75**, 4516 (1995).

²¹R. Nideröst, R. Frassanito, M. Saalfrank, A. C. Mota, G. Blatter,

- V. N. Zavaritsky, T. W. Li, and P. H. Kes, *Phys. Rev. Lett.* **81**, 3231 (1998).
- ²²M. S. Pambianchi, C. Kwon, T. Venkatesan, and S. M. Anlage, *Phys. Rev. B* **54**, 15 513 (1996).
- ²³Z. Ma, R. C. Taber, A. Kapitulnik, M. R. Beasley, P. Merchenat, C. B. Eom, S. Y. Hou, and J. M. Philips, *Phys. Rev. Lett.* **71**, 781 (1993).
- ²⁴G. Deutscher, *Nature (London)* **397**, 410 (1999).
- ²⁵R. Nemetschek, M. Opel, C. Hoffmann, P. F. Mueller, R. Hackl, H. Berger, L. Forró, A. Erb, and E. Walker, *Phys. Rev. Lett.* **78**, 4837 (1997).
- ²⁶S. Sinha and K. W. Ng, *Phys. Rev. Lett.* **80**, 1296 (1998).
- ²⁷B. Rakvin, T. A. Mahl, A. S. Bhalla, Z. Z. Sheng, and N. S. Dalal, *Phys. Rev. B* **41**, 769 (1990).
- ²⁸D. R. Harshman, R. N. Kleiman, M. Inui, G. P. Espinosa, D. B. M. A. Kapitulnik, T. Pfiz, and D. L. Williams, *Phys. Rev. Lett.* **67**, 3152 (1991).
- ²⁹V. G. Kogan, M. Ledvij, A. Y. Simonov, J. H. Cho, and D. C. Johnston, *Phys. Rev. Lett.* **70**, 1870 (1993).
- ³⁰G. Villard, D. Pelloquin, and A. Maignan, *Phys. Rev. B* **58**, 15 231 (1998).
- ³¹V. F. Correa, E. E. Kaul, and G. Nieva, *Phys. Rev. B* **63**, 172505 (2001).
- ³²Y. J. Uemura, G. M. Luke, B. J. Sternlieb, J. H. Brewer, J. F. Carolan, W. N. Hardy, R. Kadono, J. R. Kempton, R. F. Kiefl, S. R. Kreitzman, P. Mulhern, T. M. Riesman, D. Li. Williams, B. X. Yang, S. Uchida, H. Takagi, J. Gopalakrishnan, A. W. Sleight, M. A. Subramanian, C. L. Chien, M. Z. Cieplak, Gang Xiao, V. Y. Lee, B. W. Statt, C. E. Stronach, W. J. Kossler, and X. H. Yu, *Phys. Rev. Lett.* **62**, 2317 (1989).
- ³³C. Bernhard, C. Niedermayer, U. Binninger, A. Hofer, C. Wenger, J. L. Tallon, G. V. M. Williams, E. J. Ansaldo, J. I. Budnick, C. E. Stronach, D. R. Noakes, and M. A. Blankson-Millis, *Phys. Rev. B* **52**, 10 488 (1995).
- ³⁴J. P. Locquet, Y. Jaccard, A. Cretton, E. J. Williams, F. Arrouy, E. Machler, T. Schneider, O. Fischer, and P. Martinoli, *Phys. Rev. B* **54**, 7481 (1996).
- ³⁵T. Oki, N. Tsuda, and D. Shimada, *Physica C* **353**, 213 (2001).
- ³⁶X. Zhao, X. Sun, X. Fan, W. Wu, X.-G. Li, S. Guo, and Z. Zhao, *Physica C* **307**, 265 (1998).
- ³⁷A. J. Millis, S. M. Girvin, L. B. Ioffe, and A. I. Larkin, *J. Phys. Chem. Solids* **59**, 1742 (1998).
- ³⁸J. Mesot, M. R. Norman, H. Ding, M. Renderia, J. C. Campuzano, A. Paramekanti, H. M. Fretell, A. Kaminski, T. Takeuchi, T. Yokoya, T. Sato, T. Takahashi, T. Mochiku, and K. Kadowaki, *Phys. Rev. Lett.* **83**, 840 (1998).
- ³⁹V. J. Emery and S. A. Kivelson, *Phys. Rev. Lett.* **74**, 3253 (1995).
- ⁴⁰E. Roddick and D. Stroud, *Phys. Rev. Lett.* **74**, 1430 (1995).
- ⁴¹M. W. Coffey, *Physica C* **235-240**, 1961 (1995).
- ⁴²G. Lamura, J.-C. Villégier, A. Gauzzi, J. L. Cochech, J.-Y. Laval, B. Plaçais, N. Hadacek, and J. Bok, *Phys. Rev. B* **65**, 104507 (2002).
- ⁴³B. K. Chakraverty, *Physica C* **341-348**, 75 (2000).
- ⁴⁴L. Benfatto, S. Caprara, C. Castellani, A. Paramekanti, and M. Randeria, *Phys. Rev. B* **63**, 174513 (2001).
- ⁴⁵A. Gauzzi (private communication).
- ⁴⁶S. Watauchi, H. Ikuta, H. Kobayashi, J. Shimoyama, and K. Kishio, *Phys. Rev. B* **64**, 064520 (2001).
- ⁴⁷M. Tinkham, *Introduction to Superconductivity* (McGraw-Hill, New York, 1996).
- ⁴⁸D. V. Shovkun, M. R. Trunin, A. A. Zhukov, Y. A. Nefyodov, N. Bontemps, H. Enriquez, A. Buzdin, M. Daumens, and T. Tamegai, *JETP Lett.* **71**, 92 (2000).
- ⁴⁹Z. M. Yusof, B. O. Wells, T. Valla, A. V. Fedorov, P. D. Johnson, Q. Li, S. J. C. Kendiziora, and D. G. Hinks, *Phys. Rev. Lett.* **88**, 167006 (2002).
- ⁵⁰G. Deutscher, *The Gap Symmetry and Fluctuations in High- T_c Superconductors*, edited by J. Bok, G. Deutscher, D. Pavuna, and S. A. Wolf (Plenum Press, New York, 1997), pp. 15–35, and references therein.
- ⁵¹M. Onellion, *The Gap Symmetry and Fluctuations in High- T_c Superconductors* (Ref. 50), pp. 209–228, and references therein.
- ⁵²Q. Li, K. Shibusaki, M. Suenaga, I. Shigaki, and R. Ogawa, *Phys. Rev. B* **48**, 9877 (1993).
- ⁵³L. Zhang, J. Z. Liu, and R. N. Shelton, *Phys. Rev. B* **45**, 4978 (1991).
- ⁵⁴M. Pękała, E. Mąka, D. Hu, V. Brabers, and M. Ausloos, *Phys. Rev. B* **52**, 7647 (1995).
- ⁵⁵A. Y. Rykov and T. Tamegai, *Phys. Rev. B* **63**, 104519 (2001).
- ⁵⁶I. Kosztin and A. J. Leggett, *Phys. Rev. Lett.* **79**, 135 (1997).
- ⁵⁷P. J. Hirschfeld and N. Goldenfeld, *Phys. Rev. B* **48**, 4219 (1993).
- ⁵⁸P. J. Hirschfeld, W. O. Puttika, and D. J. Scalapino, *Phys. Rev. B* **50**, 10 250 (1994).
- ⁵⁹E. Šimánek, *Solid State Commun.* **31**, 419 (1979).
- ⁶⁰E. Šimánek, *Phys. Rev. B* **22**, 459 (1980).